SUPPLEMENTARY APPENDIX

In silico modelling

The DNA-binding domain (residues 121-221) of human FOXI1 (accession number NP_036320) was modelled against the crystal structure of rat Foxa3 (hepatocyte nuclear factor-3γ/HNF-3γ)) (PDB accession code 1VTN)[1] using HHPred[2] and Modeller[3] software. Homology model figures were prepared using PyMOL (http://www.pymol.org/). Consistent with protein sequence alignments (Fig. S1), identical results were obtained using the crystal structures of FOXM1,[4] FOXO4,[5] FOXK2,[6] and Foxd3[7] (Fig. S2). It should be noted that predicted position of the FOXI1 R213 residue was specific to the Foxa3 homology model since this region of the wing 2 domain in the other structures used for modelling was either not resolved or captured in contact with the DNA. Interestingly, a similar missense mutation (p.R169P) in FOXC1 has been shown to disrupt DNA binding and transcriptional activation.[8] Sequence analysis predicts FOXC1 R169 occupies a homologous position to FOXI1 R214, just one residue downstream of FOXI R213 (Fig. S1), thereby providing further evidence for the functional importance of this domain.

Plasmid constructs

Full length FOXI1 coding sequence was previously cloned into the expression vector pcDNA3.1.[9] FOXI1 was also cloned in-frame with GFP in the expression vector pEGFP-N3 (Clontech, USA), to make FOXI1-GFP fusion protein. Mutant FOXI1 L146F and R213P were generated by site-directed mutagenesis using Quikchange Lightning Site-directed mutagenesis kit (Agilent Technologies, USA) using the following primers (mutations underlined):

FOXI1 p.L146F FWD 5'-ATCTGGCTGAAAGTGAGGCGCTTGTCGGGT-3';

FOXI1 p.L146F REV 5'-ACCCGACAAGCGCCTCACTTTCAGCCAGAT-3';

FOXI1 p.R213P FWD 5'-ATTTTCTCTTCCTTTTCCTGGGGAAATTTCCATTGTCGAAC-3';

FOXI1 p.R213P REV 5'-GTTCGACAATGGAAATTTCCCCAGGAAAAGGAAGAGAAAAT-3'

Promoter reporter constructs were previously generated by cloning promoter regions of ATP6V0A4,[10] AE1 (SLC4A1),[9] and pendrin (SLC26A4) [9] into pGL3 Basic vector (Promega, USA). The sequence of each construct was verified by Sanger sequencing performed by GATC Biotech Ltd (Germany).

Cell culture, transfections, and luciferase assay

Human embryonic kidney (HEK) cell line 293T (ATCC® CRL-3216™) was maintained on gelatin coated flasks in Dulbecco's Modified Eagle medium (DMEM, Thermo Fisher Scientific, USA; 41965-039) supplemented with 10% fetal bovine serum (Thermo Fisher Scientific, USA; 16140-071) and 1 mM sodium pyruvate (Thermo Fisher Scientific, USA; 11360-039). Transient transfections were performed using Lipofectamine 2000 transfection reagent (Thermo Fisher Scientific, USA; 11668-019) according to manufacturer's protocol.

For luciferase assays, cells 90-100% confluence were trypsinized, added to a DNA/Lipofectamine mix in Opti-MEM® I Reduced Serum Medium (Thermo Fisher Scientific, USA; 31985-070) and then plated, in triplicate, with dilution approximately 1:1, into gelatin coated 96-well plates (Sarstedt, Germany; 83.1835.300). Cells were co-transfected with 0, 15, 30 or 75 ng of FOXI1 expression plasmid and 25 ng of the luciferase promoter constructs for ATP6V0A4, AE1 (SLC4A1) or pendrin (SLC26A4). Renilla luciferase plasmid (20 pg) pRL-SV40 (Promega, USA; E2231) was used to control for transfection efficiency. Empty pcDNA3.1 plasmid was used to equalize the total amount of DNA added to 100 ng/well.

Two days after transfection cells were assayed using Dual-Luciferase® Reporter Assay System (Promega, USA; E1910) according to manufacturer's protocol. Briefly, culture medium was removed and 25 µl of Passive Lysis Buffer was added to each well. Cells were then incubated at room temperature with slow rocking for 30 minutes where after 20 µl of lysate from each well was transferred to corresponding wells of a white 96-well plate (Greiner, Austria; Cat. No.: 655075) for the analysis, which was performed on a Tecan infinite M200 plate reader. Results were calculated as the quotient between values for luciferase and values for Renilla luciferase, all normalized to values for 0 ng FOXI1 expression plasmid. For intracellular distribution analysis HEK 293T cells, seeded in 24-well plates on gelatin-coated glass coverslips, were transfected with 500 ng/well of pEGFP-N3 plasmids containing wild type, L146F or R213P FOXI1 or no insert (empty vector). Two days after transfection, cells were fixed for 15 min in 4% paraformaldehyde in PBS, permeabilized in 0.1% Triton X-100 in PBS for 5 min and incubated at room temperature for 30 min with fluorescent nuclear marker To-PRO-3 (Thermo Fisher Scientific, USA; T3605). After subsequent washes in PBS, coverslips were mounted with ProLong Diamond Antifade Mountant (Thermo Fisher Scientific, USA; P36961). Imaging of GFP and To-PRO-3 signals was performed using a Zeiss LSM500 Meta system.

Western blot

HEK 293T cells were lysed in RIPA buffer (50 mM Tris-HCl, pH 8.0, 1 mM EDTA, 1% NP-40, 0.1% sodium deoxycholate, 0.1% SDS, 150 mM NaCl), supplemented with cOmplete™, EDTA-free Protease Inhibitor Cocktail (Roche, Switzerland) according to the manufacturer's recommendations. Proteins, from either cell lysates or *in vitro* translation/transcription, were separated by SDS-PAGE on NuPAGE Novex 4-12% Bis-Tris protein gels (Thermo Fisher

Scientific, USA) and transferred to PVDF membrane (Millipore, USA). FOXI1 protein was detected with polyclonal goat antibody (ab20454, Abcam, UK) diluted 1:500 in blocking buffer (5% (w/v) skim milk powder, 50 mM Tris-Cl, pH 7.5, 150 mM NaCl, 0.02% (v/v) Tween20) followed by horseradish peroxidase (HRP)-coupled polyclonal rabbit anti-goat IgG (Dako, Denmark) diluted 1:2000 in blocking buffer. HRP-coupled β-actin monoclonal mouse antibody (ab20272, Abcam, UK), diluted 1:5000 in blocking buffer, was used as a loading control of cell lysates. HRP-coupled antibody was visualized with SuperSignal West Dura Chemiluminescent Substrates (Thermo Fisher Scientific, USA) on a LAS-4000 Luminescent Image analyzer (FujiFilm, Japan).

Electrophoretic mobility shift assay (EMSA)

In vitro transcription/translations were performed according to the manufacturer's protocol using TNT® T7 Quick Coupled Transcription/Translation System (Promega, USA) and 1 µg expression plasmid. Oligonucleotides, previously shown to have binding affinity for wild type FOXI1 protein,[11] were annealed and labeled using Klenow polymerase (Roche, Switzerland) and [α-^{32}P]dCTP (PerkinElmer, USA). For each binding reaction 400000 CPM of labeled probe was incubated with 3 µl of *in vitro* translated FOXI1 protein and 1 µg of poly dI:dC in binding buffer (5 mM HEPES, 23% glycerol, 1.5 mM MgCl2, 0.2 mM EDTA, 0.5 mM DTT, 100 mM KCl) supplemented with cOmplete™, EDTA-free Protease Inhibitor Cocktail (Roche, Switzerland) at room temperature for 30 min. To the reactions Native Tris-Glycine Sample buffer (2X) was added and samples were resolved on Novex™ 6% Tris-Glycine Mini Gel and run the gel at 125 V in Novex™ Tris-Glycine Native Running Buffer (Thermo Fisher Scientific, USA). After electrophoresis, the gel was dried using a Gel Dryer Model 583 (Bio-Rad, USA), in combination with HydroTech Vacuum Pump (Bio-Rad, USA), for 2 h at 80° C and exposed to

BAS image plate (FujiFilm, Japan). The BAS image plate was subsequently scanned using FLA-7000 scanner (FujiFilm, Japan).

SUPPLEMENTARY FIGURES

Figure S1.

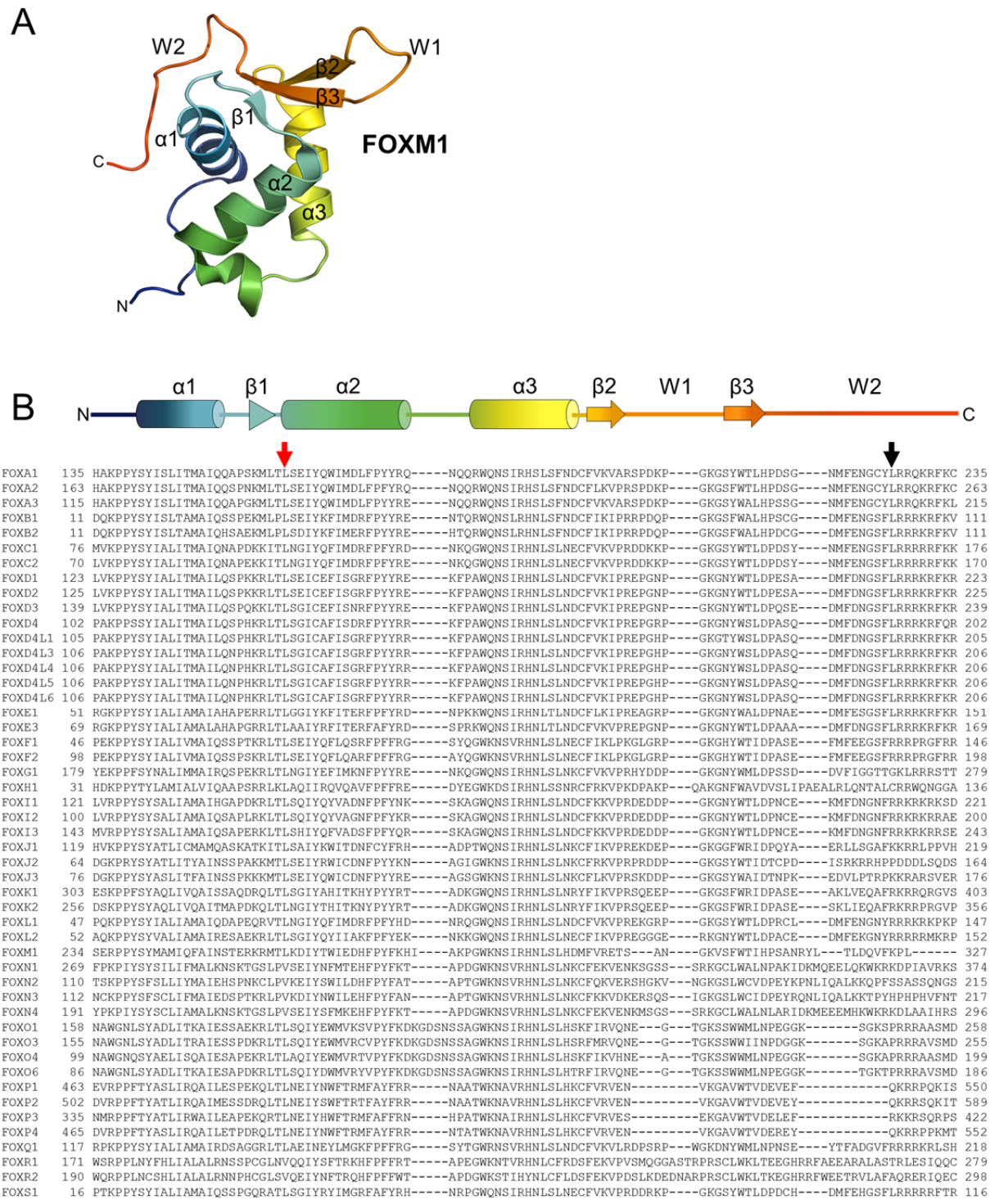


```
FOXA1   135 HAKPPYSYISLITMAIQQAPSKMLTLSEIYQWIMDLFPYYRQ-----NQQRWQNSIRHSLSFNDCFVKVARSPDKP----GKGSYWTLHPDSG----NMFENGCYLRRQKRFKC 235
FOXA2   163 HAKPPYSYISLITMAIQQSPNKMLTLSEIYQWIMDLFPFYRQ-----NQQRWQNSIRHSLSFNDCFLKVPRSPDKP----GKGSFWTLHPDSG----NMFENGCYLRRQKRFKC 263
FOXA3   115 HAKPPYSYISLITMAIQQAPGKMLTLSEIYQWIMDLFPYYRE-----NQQRWQNSIRHSLSFNDCFVKVARSPDKP----GKGSYWALHPSSG----NMFENGCYLRRQKRFKL 215
FOXB1    11 DQKPPYSYISLTAMAIQSSPEKMLPLSEIYKFIMDRFPYYRE-----NTQRWQNSLRHNLSFNDCFIKIPRRPDQP----GKGSFWALHPSCG----DMFENGSFLRRRKRFKV 111
FOXB2    11 DQKPPYSYISLTAMAIQHSAEKMLPLSDIYKFIMERFPYYRE-----HTQRWQNSLRHNLSFNDCFIKIPRRPDQP----GKGSFWALHPDCG----DMFENGSFLRRRKRFKV 111
FOXC1    76 MVKPPYSYIALITMAIQNAPDKKITLNGIYQFIMDRFPFYRD-----NKQGWQNSIRHNLSLNECFVKVPRDDKKP----GKGSYWTLDPDSY----NMFENGSFLRRRRFKK 176
FOXC2    70 LVKPPYSYIALITMAIQNAPEKKITLNGIYQFIMDRFPFYRE-----NKQGWQNSIRHNLSLNECFVKVPRDDKKP----GKGSYWTLDPDSY----NMFENGSFLRRRRFKK 170
FOXD1   123 LVKPPYSYIALITMAILQSPKKRLTLSEICEFISGRFPYYRE-----KFPAWQNSIRHNLSLNDCFVKIPREPGNP----GKGNYWTLDPESA----DMFDNGSFLRRRKRFKR 223
FOXD2   125 LVKPPYSYIALITMAILQSPKKRLTLSEICEFISGRFPYYRE-----KFPAWQNSIRHNLSLNDCFVKIPREPGNP----GKGNYWTLDPESA----DMFDNGSFLRRRKRFKR 225
FOXD3   139 LVKPPYSYIALITMAILQSPQKKLTLSGICEFISNRFPYYRE-----KFPAWQNSIRHNLSLNDCFVKIPREPGNP----GKGNYWTLDPQSE----DMFDNGSFLRRRKRFKR 239
FOXD4   102 PAKPPSSYIALITMAILQSPHKRLTLSGICAFISDRFPYYRR-----KFPAWQNSIRHNLSLNDCFVKIPREPGRP----GKGNYWSLDPASQ----DMFDNGSFLRRRKRFQR 202
FOXD4L1 105 PAKPPYSYIALITMAILQSPHKRLTLSGICAFISGRFPYYRR-----KFPAWQNSIRHNLSLNDCFVKIPREPGHP----GKGTYWSLDPASQ----DMFDNGSFLRRRKRFKR 205
FOXD4L3 106 PAKPPYSYIALITMAILQNPHKRLTLSGICAFISGRFPYYRR-----KFPAWQNSIRHNLSLNDCFVKIPREPGHP----GKGNYWSLDPASQ----DMFDNGSFLRRRKRFKR 206
FOXD4L4 106 PAKPPYSYIALITMAILQNPHKRLTLSGICAFISGRFPYYRR-----KFPAWQNSIRHNLSLNDCFVKIPREPGHP----GKGNYWSLDPASQ----DMFDNGSFLRRRKRFKR 206
FOXD4L5 106 PAKPPYSYIALITMAILQNPHKRLTLSGICAFISGRFPYYRR-----KFPAWQNSIRHNLSLNDCFVKIPREPGHP----GKGNYWSLDPASQ----DMFDNGSFLRRRKRFKR 206
FOXD4L6 106 PAKPPYSYIALITMAILQNPHKRLTLSGICAFISGRFPYYRR-----KFPAWQNSIRHNLSLNDCFVKIPREPGHP----GKGNYWSLDPASQ----DMFDNGSFLRRRKRFKR 206
FOXE1    51 RGKPPYSYIALIAMAIAHAPERRLTLGGIYKFITERFPFYRD-----NPKKWQNSIRHNLTLNDCFLKIPREAGRP----GKGNYWALDPNAE----DMFESGSFLRRRKRFKR 151
FOXE3    69 RGKPPYSYIALIAMALAHAPGRRLTLAAIYRFITERFAFYRD-----SPRKWQNSIRHNLTLNDCFVKVPREPGNP----GKGNYWTLDPAAA----DMFDNGSFLRRRKRFKR 169
FOXF1    46 PEKPPYSYIALIVMAIQSSPTKRLTLSEIYQFLQSRFPFFRG-----SYQGWKNSVRHNLSLNECFIKLPKGLGRP----GKGHYWTIDPASE----FMFEEGSFRRRPRGFRR 146
FOXF2    98 PEKPPYSYIALIVMAIQSSPSKRLTLSEIYQFLQARFPFFRG-----AYQGWKNSVRHNLSLNECFIKLPKGLGRP----GKGHYWTIDPASE----FMFEEGSFRRRPRGFRR 198
FOXG1   179 YEKPPFSYNALIMMAIRQSPEKRLTLNGIYEFIMKNFPYYRE-----NKQGWQNSIRHNLSLNKCFVKVPRHYDDP----GKGNYWMLDPSSD----DVFIGGTTGKLRRRSTT 279
FOXH1    31 HDKPPYTYLAMIALVIQAAPSRRLKLAQIIRQVQAVFPFFRE-----DYEGWKDSIRHNLSSNRCFRKVPKDPAKP---QAKGNFWAVDVSLIPAEALRLQNTALCRRWQNGGA 136
FOXI1   121 LVRPPYSYSALIAMAIHGAPDKRLTLSQIYQYVADNFPFYNK-----SKAGWQNSIRHNLSLNDCFKKVPRDEDDP----GKGNYWTLDPNCE----KMFDNGNFRRKRKRKSD 221
FOXI2   100 LVRPPYSYSALIAMAIQSAPLRKLTLSQIYQYVAGNFPFYKR-----SKAGWQNSIRHNLSLNDCFKKVPRDEDDP----GKGNYWTLDPNCE----KMFDNGNFRRKRKRRAE 200
FOXI3   143 MVRPPYSYSALIAMAIQSAPERKLTLSHIYQFVADSFPFYQR-----SKAGWQNSIRHNLSLNDCFKKVPRDEDDP----GKGNYWTLDPNCE----KMFDNGNFRRKRKRRSE 243
FOXJ1   119 HVKPPYSYATLICMAMQASKATKITLSAIYKWITDNFCYFRH-----ADPTWQNSIRHNLSLNKCFIKVPREKDEP----GKGGFWRIDPQYA----ERLLSGAFKKRRLPPVH 219
FOXJ2    64 DGKPRYSYATLITYAINSSPAKKMTLSEIYRWICDNFPYYKN-----AGIGWKNSIRHNLSLNKCFRKVPRPRDDP----GKGSYWTIDTCPD----ISRKRRHPPDDDLSQDS 164
FOXJ3    76 DGKPPYSYASLITFAINSSPKKKMTLSEIYQWICDNFPYYRE-----AGSGWKNSIRHNLSLNKCFLKVPRSKDDP----GKGSYWAIDTNPK----EDVLPTRPKKRARSVER 176
FOXK1   303 ESKPPFSYAQLIVQAISSAQDRQLTLSGIYAHITKHYPYYRT-----ADKGWQNSIRHNLSLNRYFIKVPRSQEEP----GKGSFWRIDPASE----AKLVEQAFRKRRQRGVS 403
FOXK2   256 DSKPPYSYAQLIVQAITMAPDKQLTLNGIYTHITKNYPYYRT-----ADKGWQNSIRHNLSLNRYFIKVPRSQEEP----GKGSFWRIDPASE----SKLIEQAFRKRRPRGVP 356
FOXL1    47 PQKPPYSYIALIAMAIQDAPEQRVTLNGIYQFIMDRFPFYHD-----NRQGWQNSIRHNLSLNDCFVKVPREKGRP----GKGSYWTLDPRCL----DMFENGNYRRRKRKPKP 147
FOXL2    52 AQKPPYSYVALIAMAIRESAEKRLTLSGIYQYIIAKFPFYEK-----NKKGWQNSIRHNLSLNECFIKVPREGGGE----RKGNYWTLDPACE----DMFEKGNYRRRRRMKRP 152
FOXM1   234 SERPPYSYMAMIQFAINSTERKRMTLKDIYTWIEDHFPYFKHI----AKPGWKNSIRHNLSLHDMFVRETS---AN----GKVSFWTIHPSANRYL---TLDQVFKPL------ 327
FOXN1   269 FPKPIYSYSILIFMALKNSKTGSLPVSEIYNFMTEHFPYFKT-----APDGWKNSVRHNLSLNKCFEKVENKSGSS---SRKGCLWALNPAKIDKMQEELQKWKRKDPIAVRKS 374
FOXN2   110 TSKPPYSFSLLIYMAIEHSPNKCLPVKEIYSWILDHFPYFAT-----APTGWKNSVRHNLSLNKCFQKVERSHGKV---NGKGSLWCVDPEYKPNLIQALKKQPFSSASSQNGS 215
FOXN3   112 NCKPPYSFSCLIFMAIEDSPTKRLPVKDIYNWILEHFPYFAN-----APTGWKNSVRHNLSLNKCFKKVDKERSQS---IGKGSLWCIDPEYRQNLIQALKKTPYHPHPHVFNT 217
FOXN4   191 YPKPIYSYSCLIAMALKNSKTGSLPVSEIYSFMKEHFPYFKT-----APDGWKNSVRHNLSLNKCFEKVENKMSGS---SRKGCLWALNLARIDKMEEEMHKWKRKDLAAIHRS 296
FOXO1   158 NAWGNLSYADLITKAIESSAEKRLTLSQIYEWMVKSVPYFKDKGDSNSSAGWKNSIRHNLSLHSKFIRVQNE---G---TGKSSWWMLNPEGGK-------SGKSPRRRAASMD 258
FOXO3   155 NAWGNLSYADLITRAIESSPDKRLTLSQIYEWMVRCVPYFKDKGDSNSSAGWKNSIRHNLSLHSRFMRVQNE---G---TGKSSWWIINPDGGK-------SGKAPRRRAVSMD 255
FOXO4    99 NAWGNQSYAELISQAIESAPEKRLTLAQIYEWMVRTVPYFKDKGDSNSSAGWKNSIRHNLSLHSKFIKVHNE---A---TGKSSWWMLNPEGGK-------SGKAPRRRAASMD 199
FOXO6    86 NAWGNLSYADLITKAIESAPDKRLTLSQIYDWMVRYVPYFKDKGDSNSSAGWKNSIRHNLSLHTRFIRVQNE---G---TGKSSWWMLNPEGGK-------TGKTPRRRAVSMD 186
FOXP1   463 EVRPPFTYASLIRQAILESPEKQLTLNEIYNWFTRMFAYFRR-----NAATWKNAVRHNLSLHKCFVRVEN---------VKGAVWTVDEVEF-----------QKRRPQKIS 550
FOXP2   502 DVRPPFTYATLIRQAIMESSDRQLTLNEIYSWFTRTFAYFRR-----NAATWKNAVRHNLSLHKCFVRVEN---------VKGAVWTVDEVEY-----------QKRRSQKIT 589
FOXP3   335 NMRPPFTYATLIRWAILEAPEKQRTLNEIYHWFTRMFAFFRN-----HPATWKNAIRHNLSLHKCFVRVES---------EKGAVWTVDELEF-----------RKKRSQRPS 422
FOXP4   465 DVRPPFTYASLIRQAILETPDRQLTLNEIYNWFTRMFAYFRR-----NTATWKNAVRHNLSLHKCFVRVEN---------VKGAVWTVDEREY-----------QKRRPPKMT 552
FOXQ1   117 RPKPPYSYIALIAMAIRDSAGGRLTLAEINEYLMGKFPFFRG-----SYTGWRNSVRHNLSLNDCFVKVLRDPSRP---WGKDNYWMLNPNSE----YTFADGVFRRRRKRLSH 218
FOXR1   171 WSRPPLNYFHLIALALRNSSPCGLNVQQIYSFTRKHFPFFRT-----APEGWKNTVRHNLCFRDSFEKVPVSMQGGASTRPRSCLWKLTEEGHRRFAEEARALASTRLESIQQC 279
FOXR2   190 WQRPPLNCSHLIALALRNNPHCGLSVQEIYNFTRQHFPFFWT-----APDGWKSTIHYNLCFLDSFEKVPDSLKDEDNARPRSCLWKLTKEGHRRFWEETRVLAFAQRERIQEC 298
FOXS1    16 PTKPPYSYIALIAMAIQSSPGQRATLSGIYRYIMGRFAFYRH-----NRPGWQNSIRHNLSLNECFVKVPRDDRKP----GKGSYWTLDPDCH----DMFEHGSFLRRRRFTR 116
```

Figure S2.

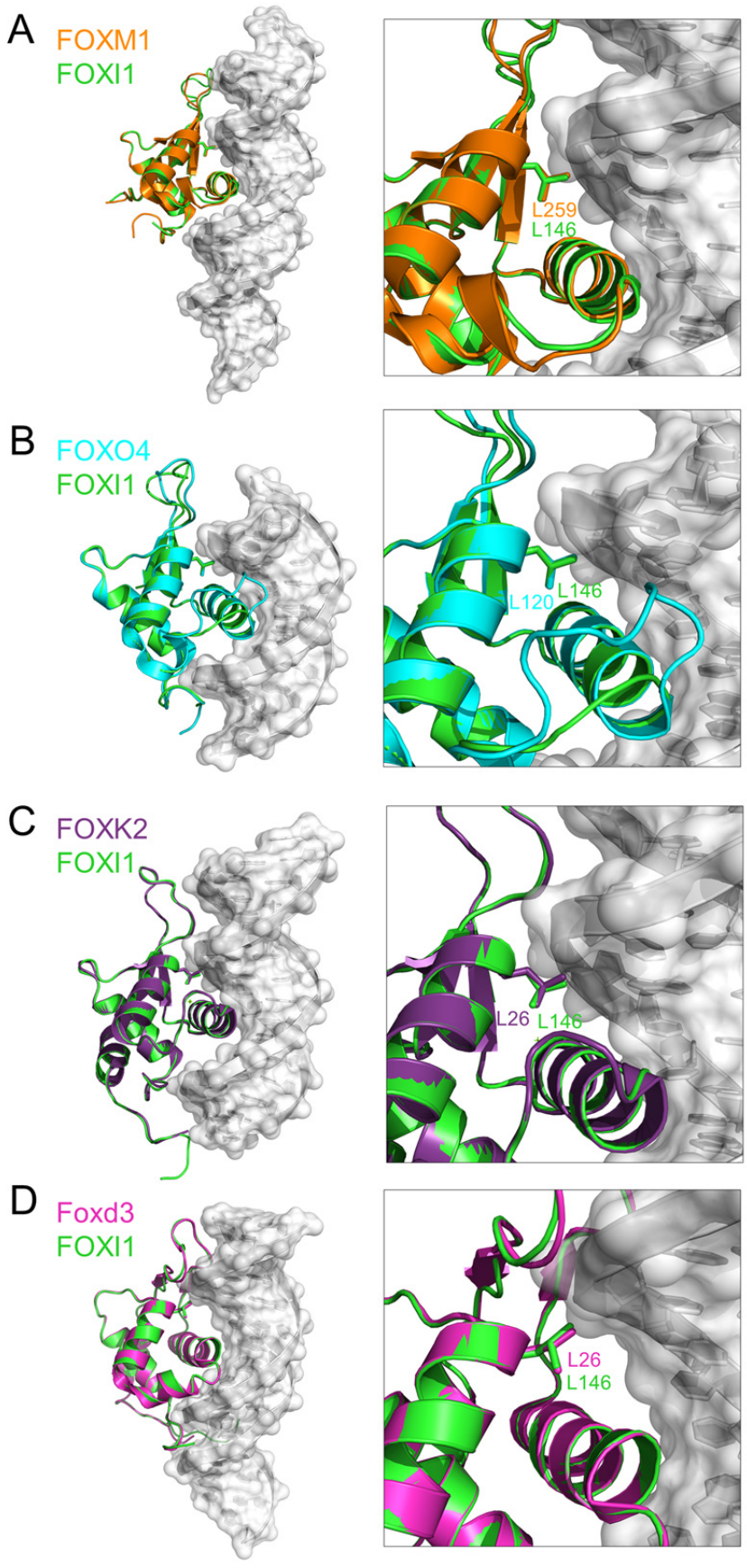
A
FOXM1
FOXI1
L259
L146
B
FOXO4
FOXI1
L120
L146
C
FOXK2
FOXI1
L26
L146
D
Foxd3
FOXI1
L26
L146

Figure S3.

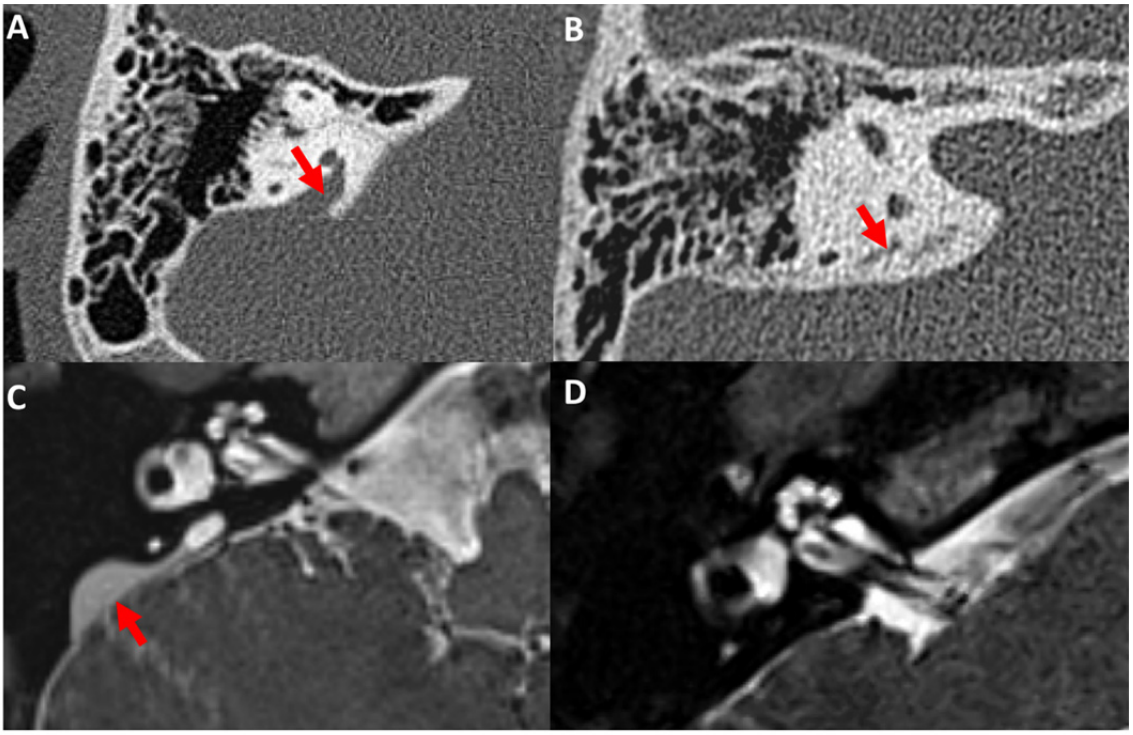

Figure S4.

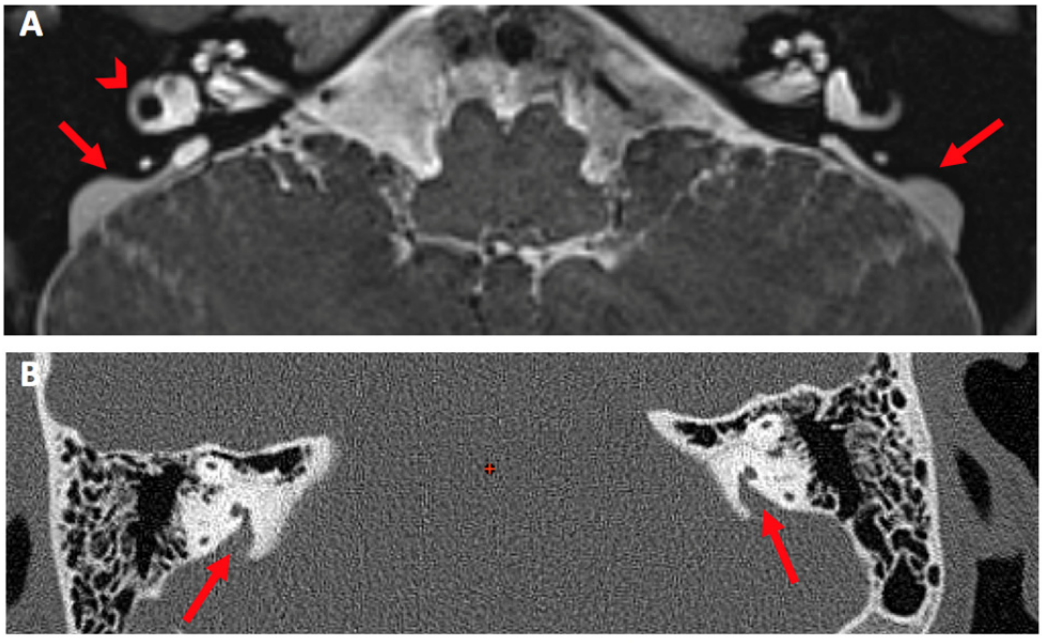

Figure S5.

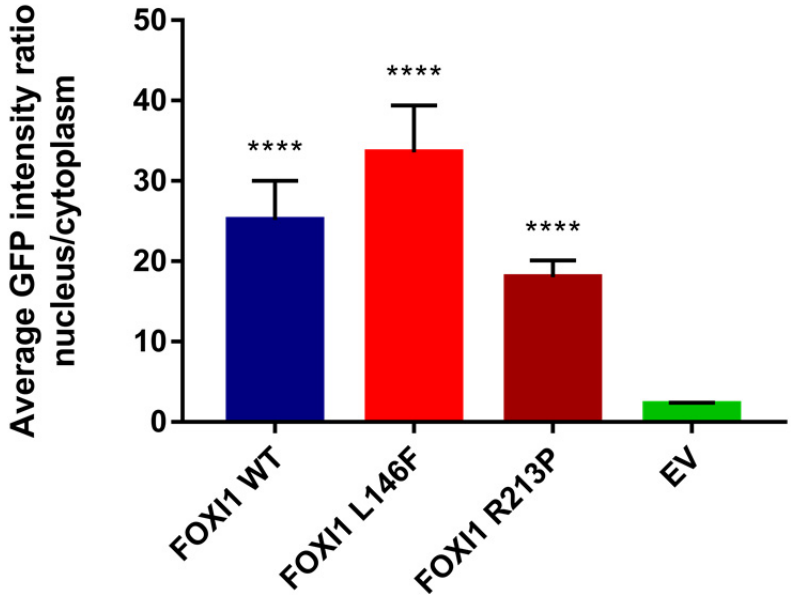

Figure S6.

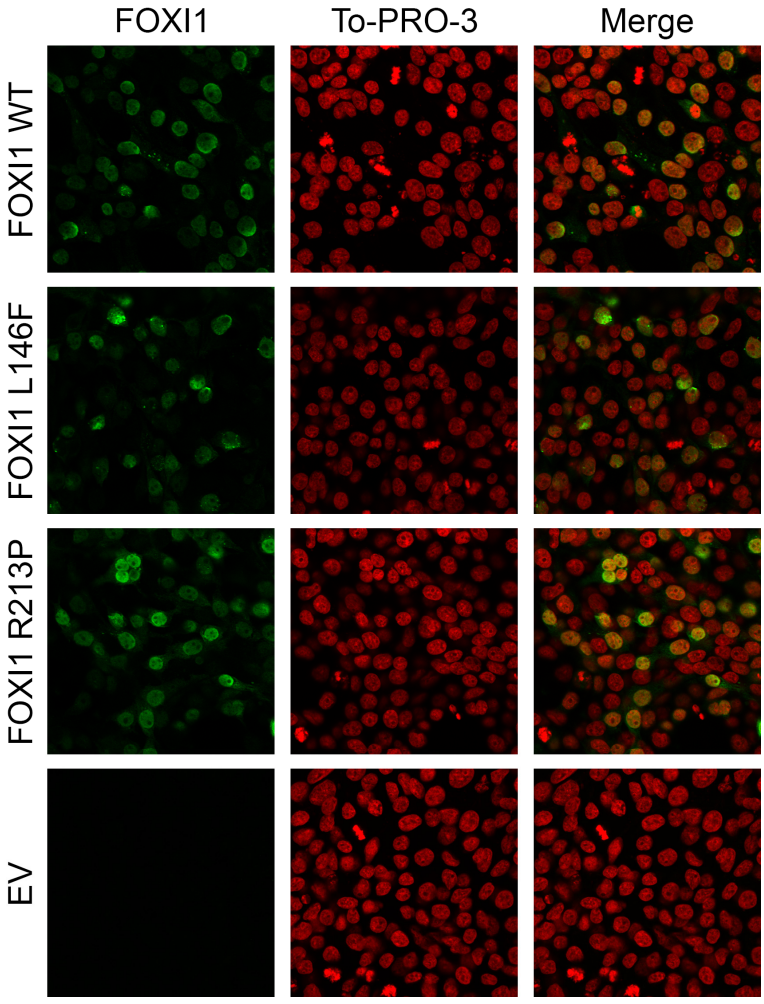

SUPPLEMENTARY FIGURE LEGENDS

Figure S1. Panel A shows the crystal structure of FOXM1 (PBD accession code 3G73)[4] colored from N-terminal (blue) to C-terminal (red) domains. Secondary structural elements are labelled: α-helices (α1-α3); β-sheets (β1-β3); and wing domains 1 and 2 (W1 and W2, respectively). Panel B shows a cartoon representation of the FOXM1 DNA-binding domain (colored as in A), depicting the approximate position of the structural elements within human FOX proteins (sequences aligned below). The position of FOXI1 L146 in α2 and FOXI1 R213 in W2 are highlighted by red and black arrows, respectively.

Figure S2. Homology modelling results for FOXI1 (in green) consistently identified FOXI1 L146 as occupying an identical position to functionally important leucine residues (numbered as in the reports) in the structures of FOXM1 (panel A, in orange; PDB code 3G73), FOXO4 (panel B, in cyan; PDB code 3L2C), FOXK2 (panel C, in purple; PDB code 2C6Y) and Foxd3 (panel D, in magenta; PDB code 2HDC). Note that the region of the wing 2 domain (W2) wherein FOXI1 R213 resides was not either not resolved in these structures (FOXM1 and FOXO4) or was not captured interacting with the target DNA (FOXK2 and Foxd3).

Figure S3. Dilatation of the vestibular aqueduct and the endolymphatic sac contained within. Shown are images of the inner ear of patient 2.1 (Panel A and C in comparison to a normal control (Panel B and D). A: High resolution CT of the petrous bones shows enlargement of the vestibular aqueduct (arrow). B. The normal vestibular aqueduct is barely visible as a small linear hypodensity (arrow). C: High resolution NMR (T2) shows dilatation of the endolymphatic sac (arrow). D: The endolymphatic sac is not visible on the NMR in the control due to its small size.

Figure S4. A: High resolution NMR (T2) shows symmetrical dilatation of the endolymphatic sac (arrows). Note that the signal of the fluid in the sacs is slightly hypointense to the signal in the lateral semicircular canals (arrowhead), due to high proteinaceous content. B: High resolution CT of the petrous bones shows corresponding enlargement of the vestibular aqueduct (arrows).

Figure S5. Determination of nuclear versus cytoplasmic GFP in 293 cells. Using ImageJ, the ratio of average GFP signal intensity in the nucleus to the average intensity in the cytoplasm of cells, (n=15 per condition), was calculated based on square-shaped equally sized regions of interest (ROIs). The results show that the ratio, considered a measure of the amount of GFP in the nucleus, was similarly and significantly higher for all three FOXI1-GFP constructs compared to the empty pEGFP-N3 plasmid (EV) (**** $p < 0.0001$). This indicates that the loss of activation of FOXI1 target genes by the two mutations is not caused by a redistribution of the FOXI1 protein. Error bars, ±sem.

Figure S6. Immunofluorescent staining of FOXI1 transfected 293 cells. 293 cells were transiently transfected with pcDNA3.1 expression plasmid carrying wild-type FOXI1 or either of the two mutated FOXI1 variants. Empty pcDNA3.1 was used as empty vector control (EV). Immunofluorescent staining with anti-FOXI1 antibody (Abcam, ab20454) showed that FOXI1 in all cases was primarily localized to the nucleus. No endogenous FOXI1 protein could be detected in empty vector control (EV). To-PRO-3 stains nuclei.

REFERENCES

1. Clark KL, Halay ED, Lai E, Burley SK. Co-crystal structure of the HNF-3/fork head DNA-recognition motif resembles histone H5. Nature 1993;364:412-20.
2. Soding J. Protein homology detection by HMM-HMM comparison. Bioinformatics 2005;21:951-60.
3. Sali A, Blundell TL. Comparative protein modelling by satisfaction of spatial restraints. Journal of molecular biology 1993;234:779-815.
4. Littler DR, Alvarez-Fernandez M, Stein A, et al. Structure of the FoxM1 DNA-recognition domain bound to a promoter sequence. Nucleic acids research 2010;38:4527-38.
5. Boura E, Rezabkova L, Brynda J, Obsilova V, Obsil T. Structure of the human FOXO4-DBD-DNA complex at 1.9 A resolution reveals new details of FOXO binding to the DNA. Acta crystallographica Section D, Biological crystallography 2010;66:1351-7.
6. Tsai KL, Huang CY, Chang CH, Sun YJ, Chuang WJ, Hsiao CD. Crystal structure of the human FOXK1a-DNA complex and its implications on the diverse binding specificity of winged helix/forkhead proteins. The Journal of biological chemistry 2006;281:17400-9.
7. Jin C, Marsden I, Chen X, Liao X. Dynamic DNA contacts observed in the NMR structure of winged helix protein-DNA complex. Journal of molecular biology 1999;289:683-90.
8. Murphy TC, Saleem RA, Footz T, Ritch R, McGillivray B, Walter MA. The wing 2 region of the FOXC1 forkhead domain is necessary for normal DNA-binding and transactivation functions. Invest Ophthalmol Vis Sci 2004;45:2531-8.
9. Blomqvist SR, Vidarsson H, Fitzgerald S, et al. Distal renal tubular acidosis in mice that lack the forkhead transcription factor Foxi1. The Journal of clinical investigation 2004;113:1560-70.
10. Vidarsson H, Westergren R, Heglind M, Blomqvist SR, Breton S, Enerback S. The forkhead transcription factor Foxi1 is a master regulator of vacuolar H-ATPase proton pump subunits in the inner ear, kidney and epididymis. PloS one 2009;4:e4471.
11. Blomqvist SR, Vidarsson H, Soder O, Enerback S. Epididymal expression of the forkhead transcription factor Foxi1 is required for male fertility. The EMBO journal 2006;25:4131-41.